The $\gamma n \to \pi^- p$ Process from ^{2}H, and ^{12}C and the $\gamma p \to \pi^+ n$ Reaction
(A Hall A Collaboration Experiment)

B. Clasie, C. Crawford, D. Dutta(Spokesperson), H. Gao(Spokesperson), B. Ma,
C.J. Seely, C.F. Williamson, H. Xiang, F. Xiong, W. Xu, L. Zhu,
MASSACHUSETTS INSTITUTE OF TECHNOLOGY

J. Arrington, F. Dohrmann, K. Hafidi, D.F. Geesaman, R.J. Holt(Spokesperson),
H.E. Jackson, D. H. Potterveld, P. E. Reimer, K. Wijesooriya,
ARGONNE NATIONAL LABORATORY

T. Averett, K. Kramer, V. Sulkosky,
COLLEGE OF WILLIAM and MARY

M. Coman, P. Markowitz,
FLORIDA INTERNATIONAL UNIVERSITY

P. Jain,
INDIAN INSTITUTE OF TECHNOLOGY, KANPUR

R. E. Segel,
NORTHWESTERN UNIVERSITY

S. Dieterich, C. Glashausser, R. Gilman, X.D. Jiang, G. Kumbartzki, R.D. Ransome,
S. Strauch,
RUTGERS UNIVERSITY

Z.-E. Meziani,
TEMPLE UNIVERSITY

J.P. Chen, E. Chudakov, J. Gomez, J.-O. Hansen, D. Higinbotham,
C.W. de Jager,J. LeRose, K. McCormick,
R. Michaels, S. Nanda, B. Reitz, A. Saha, B. Wojtsekhowski,
THOMAS JEFFERSON NATIONAL ACCELERATOR FACILITY

D. Gaskell, E.R. Kinney,
UNIVERSITY OF COLORADO

J. Ralston,
UNIVERSITY OF KANSAS

E.J. Beise,
UNIVERSITY OF MARYLAND

J. Calarco,
UNIVERSITY OF NEW HAMPSHIRE

N. Liyanage
UNIVERSITY OF VIRGINIA

Abstract

The $\gamma n \to \pi^- p$ and $\gamma p \to \pi^+ n$ reactions are essential probes of the transition from meson-nucleon degrees of freedom to quark-gluon degrees of freedom in exclusive processes. The cross sections of these processes are also advantageous, for investigation of the oscillatory behavior around the quark counting prediction, since they decrease relatively slower with energy compared with other photon-induced processes. Moreover, these photoreactions in nuclei can probe the QCD nuclear filtering effects. We propose to perform singles $\gamma p \to \pi^+ n$ measurement from hydrogen, and coincidence $\gamma n \to \pi^- p$ differential cross section measurement at the quasifree kinematics from deuterium and ^{12}C for photon energies between 2.25 GeV to 5.8 GeV at a center-of-mass angle of 90°. The proposed measurement will be carried out in Hall A using a 50 μA electron beam impinging on a 6% copper radiator, a liquid hydrogen, a liquid deuterium and a solid ^{12}C target, and the two Hall A HRS spectrometers. Nuclear transparency of the $\gamma n \to \pi^- p$ process from ^{12}C will be tested, in conjunction with exploring the nuclear dependence of rather mysterious oscillations with energy that previous experiments have indicated. The various nuclear and perturbative QCD approaches, ranging from Glauber theory, to quark-counting, to Sudakov-corrected independent scattering, make dramatically different predictions for the experimental outcomes.

I. INTRODUCTION

Exclusive processes are essential to studies of transitions from the non-perturbative to perturbative regime of QCD. The differential cross sections for many exclusive reactions [1] at high energy and large momentum transfer appear to obey the quark counting rule [2]. The quark counting rule was originally obtained based on dimensional analysis of typical renormalizable theories. The same rule was later obtained in a short-distance perturbative QCD approach by Brodsky and Lepage [3]. Despite many successes, a model-independent test of the approach, called the hadron helicity conservation rule, tends not to agree with data in the similar energy and momentum region. The presence of helicity-violating amplitudes indicates that the short-distance expansion cannot be the whole story. In addition some of the cross-section data can also be explained in terms of non-perturbative calculations [4].

In recent years, a renewed trend has been observed in deuteron photo-disintegration experiments at SLAC and JLab [5] - [7]. Onset of the scaling behavior has been observed in deuteron photo-disintegration [7] at a surprisingly low momentum transfer of 1.0 $(\mathrm{GeV/c})^2$ to the nucleon. However, a polarization measurement on deuteron photo-disintegration [8], recently carried out in Hall A at JLab, shows disagreement with hadron helicity conservation in the same kinematic region where the quark counting behavior is apparently observed. These paradoxes make it essential to understand the exact mechanism governing the early onset of scaling behavior.

Moreover, it is important to look closely at claims of agreement between the differential cross section data and the quark counting prediction. Historically, the elastic proton-proton (pp) scattering at high energy and large momentum transfer has played a very important role.

In fact, the re-scaled 90° center-of-mass pp elastic scattering data, $s^{10}\frac{d\sigma}{dt}$ show substantial oscillations about the power law behavior. With new high luminosity experimental facilities such as CEBAF, these oscillatory scaling behavior can be investigated with significantly improved precision. This will help identify the exact nature and the underlying mechanism responsible for the scaling behavior.

Oscillations are not restricted to the pp sector; they are also seen in πp fixed angle scattering [9]. The situation for meson photoproduction is unsettled and needs urgent investigation. Rough power-law dependence of meson photoproduction seems to agree with the constituent quark counting rule prediction [10] within experimental uncertainties; see for example Fig. 1 (upper panel) for the $\gamma\ p \to \pi^+\ n$ at $\theta_{cms} = 90°$. Yet it is not clear whether the $\gamma\, p \to \pi^0\ p$ process follows the correct counting rule prediction because discrepancies exist between different measurements. For the $\gamma\ n \to \pi^-\ p$ process, no cross section data exist above a photon energy of 2.0 GeV prior to the recent Jefferson Lab E94-104 experiment, in which cross section measurements of this process from a deuterium target up to a photon energy of 5.6 GeV have been carried out. Preliminary results indicate the constituent counting rule behavior in this channel at center-of-mass angle of 90°, for photon energies above $\sim$ 3 GeV. In addition to the $\frac{1}{s^7}$ scaling behavior, these preliminary results suggest an oscillatory behavior. These hints need to be investigated carefully, because the energy settings of E94-104 were designed only to investigate the global constituent quark counting rule behavior, and thus chosen to be rather coarse.

Oscillatory behavior is also suggested by the existing data on the $\gamma\ p \to \pi^+\ n$ channel, though large uncertainties preclude any conclusive statement. Thus, it is essential to confirm and map out such oscillatory scaling behavior, which will provide insight on the origins of the scaling behavior.

The energy and nuclear dependence of such oscillatory behavior is also crucial in the search for signatures of the nuclear filtering effect. The nuclear transparency of the $\gamma\ n \to \pi^-\ p$ process can be studied by taking the ratio of pion photoproduction yield from a nuclear target such as ^{12}C to the yield from ^{2}H. By finely mapping out the nuclear transparency over the scaling region it should be possible to test the nuclear filtering effect in a new regime.

We also note that the traditionally accepted "Glauber approximation" might be tested in the reactions under study. If the oscillations are a persistent feature of hard nucleon scattering, then established methods for obtaining the expected attenuation in nuclear targets exist. The qualitative nature of this approach is dramatically different from nuclear filtering. One way or the other, then, the experimental outcome of the scattering on the nuclear target is expected to be of interest to a wide audience.

In this experiment, we propose to measure the fixed-angle cross-section $\frac{d\sigma}{dt}$ for the $p(\gamma, \pi^+)n$ and $n(\gamma, \pi^- p)$ processes. We will also make the first photo-pion transparency measurement in the scaling region with the $n(\gamma, \pi^- p)$ process at the quasi-free kinematics on a ^{12}C target. In particular, we plan to map out the region of $\sqrt{s}$ = 2.25 - 3.41 GeV in fine steps. The resolution of this experiment is expected to conclusively test traditional nuclear models, as well as models based on QCD in the perturbative regime.

The proposal body is organized as following. Section II contains the physics motivations of the proposed measurement, Section III describes the proposed experiment, Section IV contains the beam time request, Section V talks about the collaboration backgrounds and responsibilities and Section VI is the summary.

II. PHYSICS MOTIVATIONS

A. Constituent Counting Rule and Oscillations

The constituent counting rule predicts the energy dependence of the differential cross section at fixed center-of-mass angle for an exclusive two-body reaction at high energy and large momentum transfer as follows:

$$d\sigma/dt = h(\theta_{cm})/s^{n-2}, \tag{1}$$

where s and t are the Mandelstam variables, s is the square of the total energy in the center-of-mass frame and t is the momentum transfer squared in the s channel. The quantity n is the total number of elementary fields in the initial and final states, while $h(\theta_{cm})$ depends on details of the dynamics of the process. In the case of pion photoproduction from a nucleon target, the quark counting rule predicts a $\frac{1}{s^7}$ scaling behavior for $\frac{d\sigma}{dt}$ at a fixed center-of-mass angle. The quark counting rule was originally obtained based on dimensional analysis under the assumptions that the only scales in the system are momenta and that composite hadrons can be replaced by point-like constituents. Implicit in these assumptions is the approximation that the class of diagrams, which represent on-shell independent scattering of pairs of constituent quarks (Landshoff diagrams) [11], can be neglected. These counting rules were also confirmed within the framework of perturbative QCD analysis up to a logarithmic factor of α_s and are believed to be valid at high energy, in the perturbative QCD region. Such analysis relies on the factorization of the exclusive process into a hard scattering amplitude and a soft quark amplitude inside the hadron.

Although the quark counting rule agrees with data from a variety of exclusive processes, the other natural consequence of pQCD: the helicity conservation selection rule, tends not to agree with data in the experimentally tested region. Hadron helicity conservation arises from quark helicity conservation at high energies and the vector gluon-quark coupling nature of QCD, by neglecting the higher angular momentum states of quarks or gluons in hadrons. The same dimensional analysis which predicts the quark counting rule also predicts hadron helicity conservation for exclusive processes at high energy and large momentum transfers. If hadron helicity conservation holds, the induced polarization of the recoil proton in the unpolarized deuteron photo-disintegration process is expected to be zero. A polarization measurement [8] in deuteron photo-disintegration has been carried out recently by the JLab E89-019 collaboration. While the induced polarization does seem to approach zero around a photon energy of 1.0 GeV at 90° center-of-mass angle, the polarization transfer data are inconsistent with hadron helicity conservation.

The entire subject is very controversial. Isgur and Llewellyn-Smith [4] argue that if the nucleon wave-function has significant strength at low transverse quark momenta ($k_\perp$), then the hard gluon exchange (essential to the perturbative approach) which redistributes the transfered momentum among the quarks, is no longer required. The applicability of perturbative techniques at these low momentum transfers is in serious question. There are no definitive answers to the question- *what is the energy threshold at which pQCD can be applied?* Indeed the exact mechanism governing the observed quark counting rule behavior remains a mystery. Thus, it is crucial to also look for other QCD signatures.

Apart from the early onset of scaling and the disagreement with hadron helicity conservation rule, several other striking phenomena have been observed in pp elastic scattering. One such phenomena is the oscillation of the differential cross-section about the scaling behavior predicted by the quark counting rule (s^{-10} for pp scattering), first pointed out by Hendry [12] in 1973.

Secondly, the spin correlation experiment in pp scattering first carried out at Argonne by Crabb *et al.* [13] shows striking behavior: it is ~ 4 times more likely for protons to scatter when their spins are both parallel and normal to the scattering plane than when they are anti-parallel, at the largest momentum transfers ($p_T{}^2 = 5.09$ (GeV/c)^2, $\theta_{c.m.} = 90°$). Later spin-correlation experiments [14] confirm the early observation by Crabb *et al.* [13]. Theoretical interpretation for such an oscillatory behavior ($s^{10}\frac{d\sigma}{dt}$) and the striking spin-correlation in pp scattering was attempted by Brodsky, Carlson, and Lipkin [15] within the framework of quantum chromodynamic quark and gluon interactions, where interference between hard pQCD short-distance and long-distance (Landshoff) amplitudes was discussed for the first time. The Landshoff amplitude arises due to multiple independent scattering between quark pairs in different hadrons. Although each scattering process is itself a short distance process, different independent scatterings can be far apart, limited only by the hadron size. Moreover, gluonic radiative corrections give rise to a phase to this amplitude which is calculable in pQCD [16]. This effect is believed to be analogous to the coulomb-nuclear interference that is observed in low-energy charged-particle scattering. It was also shown that at medium energies this phase (and thus the oscillation) is energy dependent [17], while becoming energy independent at asymptotically high energies [17], [18].

Lastly, Carroll *et al.* [19] reported the anomalous energy dependence of nuclear transparency from the quasi-elastic A(p,2p) process: the nuclear transparency first rises followed by a decrease. This intriguing result was confirmed recently at Brookhaven [20] with improved experimental technique in which the final-state was completely reconstructed. Ralston and Pire [21] explained the free pp oscillatory behavior in the scaled differential cross section and the A(p,2p) nuclear transparency results using the ideas of interference between the short-distance and long-distance amplitudes and the QCD nuclear filtering effect. Carlson, Chachkhunashvili, and Myhrer [22] have also applied such an interference concept to the pp scattering and have explained the pp polarization data.

It was previously thought that the oscillatory $s^{10}\frac{d\sigma}{dt}$ feature is unique to pp scattering or to hadron induced exclusive processes. However, it has been suggested that similar oscillations should occur in deuteron photo-disintegration [23], and photo-pion productions at large angles [24]. The QCD re-scattering calculation of the deuteron photo-disintegration process by Frankfurt, Miller, Sargsian and Strikman [23] predicts that the energy dependence of the differential cross-section, $s^{11}\frac{d\sigma}{dt}$ arises primarily from the $n-p$ scattering in the final state. If these predictions are correct, such oscillatory behavior may be a general feature of high energy exclusive photoreactions. Thus it is very important to experimentally search for these oscillations in photoreactions.

Farrar, Sterman and Zhang [25] have shown that the Landshoff contributions are suppressed at leading-order in large-angle photoproduction but they can contribute at sub-leading order in $\frac{1}{Q}$ as pointed out by the same authors. In principle, the fluctuation of a photon into a $q\bar{q}$ in the initial state can contribute an independent scattering amplitude at sub-leading order. However, the vector-meson dominance diffractive mechanism is already

suppressed in vector meson photoproduction at large values of t [26]. On the other hand such independent scattering amplitude can contribute in the final state if more than one hadron exist in the final state, which is the case for both the deuteron photo-disintegration and nucleon photo-pion production reactions. Thus, an unambiguous observation of such an oscillatory behavior in exclusive photoreactions with hadrons in the final state at large t may provide a signature of QCD final state interaction. The most recent data on $d(\gamma, p)n$ reaction [7] show that the oscillations, if present, are very weak in this process, and the rapid drop of the cross section ($\frac{d\sigma}{dt} \propto \frac{1}{s^{11}}$) makes it impractical to investigate such oscillatory behavior.

Given that the nucleon photo-pion production has a much larger cross-section at high energies ($\frac{d\sigma}{dt} \propto \frac{1}{s^7}$), it is very desirable to use these reactions to verify the existence of such oscillations. In fact, the existing data on $\gamma p \to \pi^+ n$ suggest oscillatory behavior but the statistical uncertainties are poor at higher energies(see Fig. 1). The preliminary $\gamma n \to \pi^- p$ (E94-104) data show hints of oscillation in the scaled differential cross-section with high statistical accuracy. However, the rather coarse beam energy settings prevent a conclusive statement about the oscillatory behavior. Thus, to verify any structure in the scaled cross-section of photo-pion production processes, it is imperative that we do a fine scan of the scaling region for the $\gamma p \to \pi^+ n$ and $\gamma n \to \pi^- p$ processes at a 90° center-of-mass angle.

B. Nuclear Filtering

Nuclear filtering refers to the suppression of the long distance amplitude (Landshoff amplitude) in the strongly interacting nuclear environment. Large quark separations tend not to propagate in the nuclear medium while small quark separations propagate with small attenuation. This leads to suppression of the oscillation phenomena arising from interference of the long distance amplitude with the short distance amplitude (as seen in pp scattering, mentioned earlier). Nuclear transparency measurements in A(p,2p) experiments carried out at Brookhaven [19] have shown a rise in transparency for $Q^2 \approx 3$ - 8 $(\mathrm{GeV/c})^2$, and a decrease in the transparency at higher momentum transfers, as shown in Fig 2. A more recent experiment [20], completely reconstructing the final-state of the A(p,2p) reaction, confirms the validity of the earlier Brookhaven experiment. If the oscillatory behavior of the cross-section is suppressed in nuclei one would expect to see oscillations in the transparency, which are 180^0 out of phase with the oscillations in the free pp cross-section. This is because the transparency is formed by dividing the A(p,2p) cross-section by the pp cross-section scaled by the proton number Z of the nuclear target. Brodsky and de Teramond [27] claimed that the structure seen in $s^{10}\frac{d\sigma}{dt}(pp \to pp)$, the A_{NN} spin correlation at $\sqrt{s} \sim 5$ GeV (around center-of-mass angle of 90°) [13], [14], and the $A(p, 2p)$ transparency result can be attributed to $c\bar{c}uuduud$ resonant states. The opening of this channel gives rise to an amplitude with a phase shift similar to that predicted for gluonic radiative corrections.

While interpretations of the elastic $pp \to pp$ cross section, the analyzing power A_{NN} and the transparency data remain controversial, the ideas of nuclear filtering effect and the interference between the hard pQCD short-distance and the long-distance Landshoff amplitudes by Ralston and Pire [21] are able to explain both the $s^{10}\frac{d\sigma}{dt}(pp \to pp)$ oscillatory behavior and the Brookhaven A(p,2p) transparency data. Carlson, Chachkhunashvili, and

Myhrer [22] have also applied such an interference concept to explain the pp polarization data.

Recently, a first complete calculation of "color transparency" and 'nuclear filtering' in perturbative QCD has been carried out for electro-production experiments [28]. These calculations show that the nuclear filtering effect is complementary to color transparency (CT) effect. Color transparency, first conjectured by Mueller and Brodsky [29] refers to the suppression of final (and initial) state interactions of hadrons with the nuclear medium in exclusive processes at high momentum transfers. The phenomenon of CT occurs when exclusive processes proceed via the selection of hadrons in the so-called point-like-configuration (PLC) states. Furthermore this small configuration should be "color screened" outside its small radius and the compact size should be maintained while it traverses the nuclear medium. While nuclear filtering uses the nuclear medium actively, in CT large momentum transfers select out the short distance amplitude which are then free to propagate through the passive nuclear medium. The expansion time relative to the time to traverse the nucleus is an essential factor for the observation of the CT effect, based on the quantum diffusion model by Farrar, Liu, Frankfurt and Strikman [30]. Thus, while one expects to observe the onset of CT effect sooner in light nuclei compared to heavier nuclei, the large A limit provides a perturbatively calculable limit for the nuclear filtering effect. This makes ^{12}C a good choice as the target for the proposed nuclear transparency measurement. The experimental verification of the nuclear filter effect would be a very interesting confirmation of this QCD based approach in the transition region. For a detailed discussion on the nuclear filtering effect and related subjects, we refer to a review article on the subject [31].

As mentioned in the introduction, oscillations are suggested by the existing cross-section data in photo-pion production reactions. Such oscillatory behavior is predicted from QCD if the independent scattering (Landshoff) regions are important. Nuclear filtering in turn should remove these regions. Thus one can investigate the nuclear filtering effect by measuring transparency in the pion photoproduction reactions as well. Fig. 3 shows the world data (upper panel) and a calculation of the scaled differential cross-section $s^7 \frac{d\sigma}{dt}$ for the $\gamma p \to \pi^+ n$, as a function of $\sqrt{s}$ at a center-of-mass angle of 90° and the calculated transparency (lower panel) of the $\gamma p \to \pi^+ n$ process as a function of $\sqrt{s}$ for heavy targets such as ^{12}C, using a two-component model of Jain, Kundu, and Ralston [24]. There are two different phases in the two-component model: the QCD energy-dependent phase due to the gluon radiation as in the free cross section, and the phase difference between the two amplitudes in the effective nuclear potentials in the nuclear medium. While the QCD phase can be determined by fitting the free cross-section, the latter phase is unknown. The results of the two-component model shown are obtained for different values of the second phase. An effective $p-N$ cross section of 30 mb is used in this calculation based on the $A(e,e'p)$ data [32], and the $\pi - N$ cross section is attenuated by $\frac{1}{Q}$ based on the pQCD calculation [28]. Although the calculation was carried out for the $\gamma p \to \pi^+ n$ channel (where free space cross-section data exists), the following features are expected for the $\gamma n \to \pi^- p$ channel as well: (i) an overall slow increase in the transparency as $\sqrt{s}$ increases; (ii) an oscillatory behavior with amplitude depending strongly on the relative phase between the effective nuclear potential of the short-distance and the long-distance amplitudes in the nuclear medium. While a relative phase angle of ZERO predicts the smallest amplitude for the oscillation, it is disfavored by the Brookhaven A(p,2p) transparency data [33].

In summary, the preliminary E94-104 results in a rather coarse step of $\sqrt{s}$, seem to suggest oscillatory behavior in $s^7 \frac{d\sigma}{dt}$. Thus, it is essential to confirm such oscillatory behavior in finer step of $\sqrt{s}$ in the $\gamma p \to \pi^+ n$ and $\gamma n \to \pi^- p$ processes. Furthermore, a nuclear transparency measurement of the $\gamma n \to \pi^- p$ process from a ^{12}C target will allow the investigation of the nuclear filtering effect.

III. PROPOSED MEASUREMENTS

We propose to carry out a measurement of the photo-pion production cross-section for the fundamental $\gamma n \to \pi^- p$ process from a ^{2}H and ^{12}C target and for the $\gamma p \to \pi^+ n$ process from a hydrogen target at a center-of-mass angle of 90^o, at $\sqrt{s} \sim 2.25$ GeV to 3.41 GeV in steps of approximately 0.07 GeV. The maximum beam energy requested is 5.8 GeV. Transparency will be formed by taking the ratio of the production cross-section from ^{12}C to the production cross-section from ^{2}H. The calculations of Jain *et al.* [24] in this region predict oscillations of the order of 30% for ^{12}C. We plan to make individual cross-section measurements with a 2% statistical uncertainty and point-to-point systematic uncertainties of $< 3\%$, which will allow the test of the oscillatory behavior in the scaled free cross section. The systematic uncertainties for the transparency measurement will be greatly reduced when we take the ratio of Carbon to ^{2}H. Thus, for transparency we plan to make measurements with combined statistical and systematic uncertainties of $< 5\%$, which should be sufficient to provide evidence for or against the nuclear filtering effect in nuclear photo-pion production processes. With combined statistical and systematic uncertainties of $<5\%$, it should be possible to confirm the Glauber predictions as well.

We request a total of 15 different beam energies in order to test the oscillatory behavior and to investigate the nuclear filtering effect. Some of the beam energies can be accommodated by changing the number of passes in the linac, still a number of changes to the energy value per pass is needed. Thus, the beam energy change is the main overhead of this experiment. In addition, frequent beam energy change at lower energies adds another level of complexity in scheduling the experiment. However, the proposed experiment is a straightforward measurement, which requires the standard Hall A equipment. Thus, interweaving the running of this experiment with the running of other compatible Hall A experiments can be a practical running scenario for the scheduling of such an experiment.

While the large acceptance detection and a tagged photon capabilities have enormous advantages for many experiments in Hall B, the proposed experiment will only be possible with the unique JLab capability of high luminosity. The proposed momentum range for the coincidence measurement of the $\gamma n \to \pi^- p$ process makes Hall A the only possible place at JLab where such a measurement can be carried out.

IV. THE EXPERIMENT

A. Overview

The experiment will employ the Hall A cryogenic liquid hydrogen and deuterium targets and the solid target ladder with a carbon foil target and the Hall A copper radiator. The

maximum energy of the bremsstrahlung beam is essentially equal to the electron kinetic energy. The target, located downstream of the radiator, is irradiated by the photons and the primary electron beam. The quasifree kinematics are chosen for the $n(\gamma, \pi^- p)$ and $p(\gamma, \pi^+)n$ processes. The singles measurement will be performed using the left-arm HRS to detect the π^+. The coincidence measurement will be performed using the Hall A right-arm HRS for the π^- detection, and the left-arm HRS for the proton detection. The detector packages for both HRS arms in this experiment will be identical to that used in the recently completed E94-104 experiment. Fig. 4 shows the experimental layout for the proposed experiment.

The $\gamma n \to \pi^- p$ reaction is a two-body process. By either detecting the momentum and the angle of the photo-proton or detecting the momentum and angle of the photo-produced pion, one can determine the incident photon energy. In this experiment, nuclear targets (deuterium and ^{12}C) will be employed instead of a free neutron target which does not exist in nature. Thus, measurement of the momenta and scattering angles of both the proton and the pion are necessary in order to reconstruct the incident photon energy. Other inelastic channel, such as 2π production can be essentially eliminated, since this is a coincidence measurement and only the highest energy protons and pions are detected. This technique has been well established in the recently completed Hall A experiment E94-104. Using the data from E94-104, we have compared the reconstructed photon energy spectrum for a ^{4}He target with Monte Carlo simulation of the same (Fig 5). The excellent agreement between the two gives us added confidence in this technique.

B. The Electron Beam and the Radiator

An electron beam with a beam current of 50 μA is required for this experiment. The experiment will use a copper radiator of 6% radiation length, which is placed upstream of the target chamber. The copper radiator constructed by the Rutgers University has been used in several completed Hall A photon experiments including the most recent E94-104 experiment.

The proposed running conditions of this experiment are very close to those of E94-104, the background from the copper radiator due to the production of low energy neutrons and high energy pions were demonstrated not to be a problem by E94-104. Another experiment, E00-107 which proposes to use a 50 μA beam has been approved by the PAC.

C. Target

We plan to use the Hall A liquid deuterium and liquid hydrogen (2% r.l. each) cryotargets and a solid target of carbon (850mg, 2% r.l.). The liquid hydrogen target will be used for the singles $\gamma p \to \pi^+ n$ measurement and for coincidence background studies. The dummy target cell will be used for singles background studies. We propose to run the experiment at a maximum electron beam current of 50 μA, which is significantly below the heat load that the Hall A cryotarget routinely handles. The energy deposited at the highest energy (5.8 GeV) with 50 μA of beam is below the 100 Watts equivalent thick target power limit.

D. Spectrometer

The two HRS spectrometers will be used to make the coincidence measurement. The right-arm HRS will be used for the π^- detection, and the left-arm HRS for the proton detection. The pion arm momentum setting ranges from 1.32 - 3.08 GeV/c and the angle ranges from 30.7 - 44.8°. The proton arm momentum and angle setting ranges from 1.61 - 3.45 GeV/c and 26.08 - 35.22°. The highest singles rate in the spectrometer is less than 5KHz, which is much lower than the limit for the trigger rate. The left-arm HRS will also be used to detect the π^+ from a hydrogen target.

E. Background

The dominant background process for this experiment is the quasi-elastic A(e,e'p) reaction. The quasielastically scattered electron has nearly the same momentum and angle as the photo-produced pion in the pion arm, and the scattered proton also has nearly the same momentum and scattering angle as that of the photo-proton in the proton spectrometer. We have estimated the singles ratio of e^-/π^- for the LH2 and LD2 targets, based on the observed ratio in the experiment E94-104. The ratio is < 10 for the LD2 target and < 50 for the LH2 target. The combination of the gas Cherenkov counter, preshower and shower counters can provide an electron rejection factor of 5000, which is sufficient for the proposed experiment. In the proton arm, good particle identification of protons, π^+ particles and positrons is required. The positron background arises from pair production of the bremsstrahlung photons and can be rejected sufficiently using the gas Cherenkov counter because the rate has been estimated to be rather low. Although the π^+ particles from the $\gamma p \to \pi^+ n$ reactions are kinematically eliminated in the proton arm, the π^+ background event can come from multiple processes, which have relatively low rates because of the phase space constraint. The combination of the A1 and A2 aerogel counters will provide more than sufficient π^+ rejection, which has been clearly demonstrated by experiment E94-104. Furthermore, the coincidence requirement effectively suppresses all background channels, except the (e,e'p) channel. Experiment E94-104 demonstrated that the coincidence (e,e'p) background events are sufficiently rejected with the particle identification capabilities provided by the detector packages shown in Fig. 4.

F. Kinematics

Tables I and II shows the kinematics for the $p(\gamma, \pi^+)n$ and and the quasifree $n(\gamma, \pi^- p)$ reactions respectively. The photon energy is taken to be 75 MeV below the electron beam energy, since the range of photon energies to be used is a 100 MeV bin from 25 MeV below the end point energy to 125 MeV below the end point energy. However since the rates are relatively high for $\sqrt{s} < 2.8$ GeV, we can divide the 100 MeV bin into two 50 MeV bins for these low $\sqrt{s}$ points. The range in $\sqrt{s} < 2.8$ GeV which is covered by splitting this 100 MeV bin is shown in Table III. The pion center-of-mass angle is 90^o at all settings. The kinematics have been chosen to cover the region between center-of-mass energy $\sqrt{s} = 2.26$ - 3.41 GeV, in steps of approximately 0.07 GeV.

G. Counting Rates

The counting rate were estimated using the data taken on the ^{2}H and ^{4}He targets during E94104 and a Monte Carlo simulation of the experiment using the Hall A Monte Carlo MCEEP modified for experiment E94-104. The Monte Carlo uses a fit to the existing data on $\gamma n \to \pi^- p$, the measured π^-/π^+ ratio from experiment E94-104 and momentum distributions for ^{2}H, ^{4}He and ^{12}C to simulate the photon energy spectrum for each target (^{1}H, ^{2}H, ^{4}He and ^{12}C respectively). The reconstructed photon energy spectrum for $\gamma n \to \pi^- p$ on a ^{4}He agrees very well with the data, as seen in Fig 5. Similarly we also performed a Monte Carlo simulation for the ^{12}C targets as shown in Fig 6. The momentum distribution for ^{12}C was obtained from Hall C experimental data [34]. Using the calculated transparency obtained from Ref [35], we can get an estimate of the relative transparency of ^{12}C with respect to ^{4}He. One can thus obtain the coincidence rates for ^{12}C from this relative transparency using the relation;

$$T_{\text{relative}} = \frac{T_{^{12}C}}{T_{^4He}} = \frac{\text{Data}(^{12}C)/\text{Monte Carlo}(^{12}C)}{\text{Data}(^4He)/\text{Monte Carlo}(^4He)} \tag{2}$$

The relative transparency between ^{12}C and ^{4}He was taken to be 0.8. All rates were estimated for a 50 MeV photon energy window for $\sqrt{s} < 2.8$ GeV and a 100 MeV photon energy window for $\sqrt{s} > 2.8$ GeV, starting 25 MeV below the end point energy. A beam current of 50 μA, a 6% copper radiator and ^{12}C target of thickness 850 mg/cm^2 was used in the estimation. Since the available E94-104 data is more coarsely spaced than this experiment, a linear extrapolation was used to estimate the rates for energies between any two E94-104 data points. The rates for the 15 cm LD2 target were determined from the E94-104 measured rates. The estimated counting rates are shown below in Table IV

The singles $d(\gamma, \pi^-)$ and $d(\gamma, p)$ rates were estimated from the observed singles rates in E94-104. The coincidence timing resolution was taken to be 2 ns in the estimation of the accidental rates. The e^-/π^- ratio was estimated from the observed ratio in experiment E94-104. The singles rates, the accidental rates and and the e^-/π^- ratio for the LD2 targets is shown in Tables V. The singles, accidentals and the e^-/π^- ratio are expected to be similar for the solid targets compared to those for the LD2 target.

H. Beam Time Estimate

Beam times requirements for data with the radiator were estimated for a goal of 2% statistical uncertainty for the LH2, LD2 and ^{12}C targets. The beam time estimates for the data without the radiator are taken to be a third of the time required with the radiator. The beam time estimates are shown below in table VI. It includes 15 hours of background studies for the coincidence measurement and 5 hours of background studies for the singles measurement. In addition to the 215 hours of beam time listed in the table, we estimate the time for beam energy change [36] for the 15 kinematic points to be an average of 6 hrs each. Thus the total overhead for beam energy change is expected to be around 90 hours. All spectrometer setting changes will take place during beam energy changes, thus there are no additional overhead for spectrometer momentum and angle changes. But for the

singles measurement, the hadron spectrometer angle and momentum changes will require an overhead of about 8 hours total for all the 15 kinematic points. The overhead for changes in target and radiator at the rate of 15 minutes for each change add up to ∼20 hours. Thus, the total overhead is expected to be 118 hours and the total time required for the experiment is 333 hours (∼ 14 days).

I. Systematic Uncertainties and Projected Results

The experience gained in E94-104 suggests that the systematic uncertainties of this kind of experiment are well under control. For the cross-section measurements the systematic uncertainties are expected to be $< 5\%$. However, the systematic uncertainty in energy dependence of the cross-section will be $< 3\%$. Since the transparency measurement is a ratio measurement, many of the spectrometer related systematic errors will cancel. We expect the net systematic uncertainty for the transparency measurement to be $< 3\%$. The projected results for LH2, LD2 and ^{12}C are shown in Fig. 7, Fig. 8 and Fig. 9. Fig. 9 also shows the calculated transparency [33] for three different phase angles of 0°, 45° and 90°. Figs 10, 11, and 12 show the projected results for $\sqrt{s} < 2.8$ GeV where the useful photon energy bin can be split to give us a much finer scan of the low $\sqrt{s} < 2.8$ GeV region. It is clear that the projected statistical and systematic uncertainties are more than sufficient to make definitive statements on the predicted oscillations in the scaled cross-section and in the ^{12}C nuclear transparency.

V. COLLABORATION BACKGROUND AND RESPONSIBILITIES

Many members of the current collaboration have been involved in a number of bremsstrahlung photon beam experiments at SLAC and JLab. Most members of the group are experienced in running the Hall-A radiator, cryotargets and spectrometers. This experiment is a follow-up of experiment E94-104 and most members had participated in that experiment as well as the Hall A photo-proton polarization experiments (E89-019 and E94-012).

VI. SUMMARY

We have proposed a measurement of the $\gamma p \to \pi^+ n$ reaction and $\gamma n \to \pi^- p$ at a center-of-mass angle of 90^o. We plan to map out the region of $\sqrt{s} = 2.25$ - 3.41 GeV in fine steps of approximately 0.07 GeV. We will also make the first photo-pion transparency measurement in the scaling region with the $n(\gamma, \pi^- p)$ process at the quasi-free kinematics on a ^{12}C target. These measurement would test the oscillatory behavior of the scaled free space differential cross-sections about the quark counting prediction. And by finely mapping out the nuclear transparency over the scaling region it should be possible to test the nuclear filtering effect in a new regime. We will use the standard Hall-A equipment along with a 6% copper radiator. The Hall-A cryogenic liquid hydrogen and liquid deuterium and a solid carbon target will be used. A total of 333 hours (∼ 14 days) of beam time will be required for this experiment.

VII. ACKNOWLEDGEMENTS

We thank G.A. Miller, M. Sargsian and T. W. Donnelly for helpful comments.

FIGURES

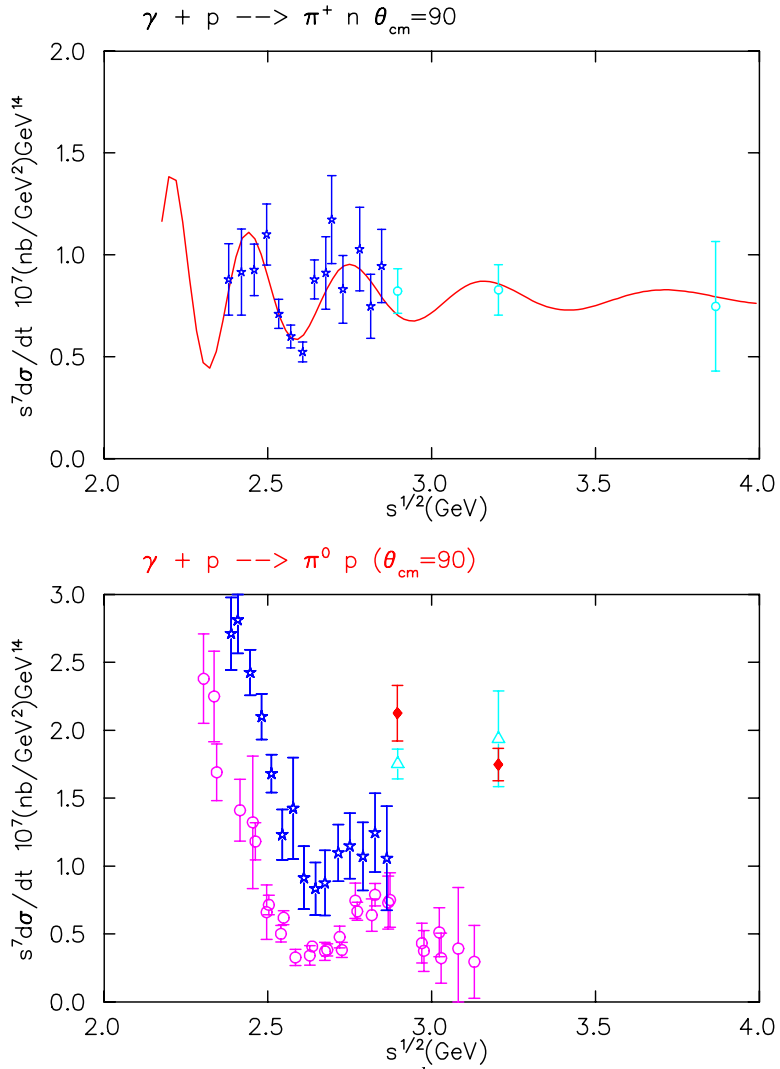

FIG. 1. The scaled differential cross section, $s^7 \frac{d\sigma}{dt}$ as a function of $\sqrt{s}$ at a center-of-mass angle of 90°. The upper panel is for the $\gamma p \to \pi^+ n$ channel and the lower panel is for the $\gamma p \to \pi^0 p$ channel. The solid curve is a fit based on the two-component model [24]. Different plotting symbols represent data from different experiments listed in [37] and the solid diamonds are from [38].

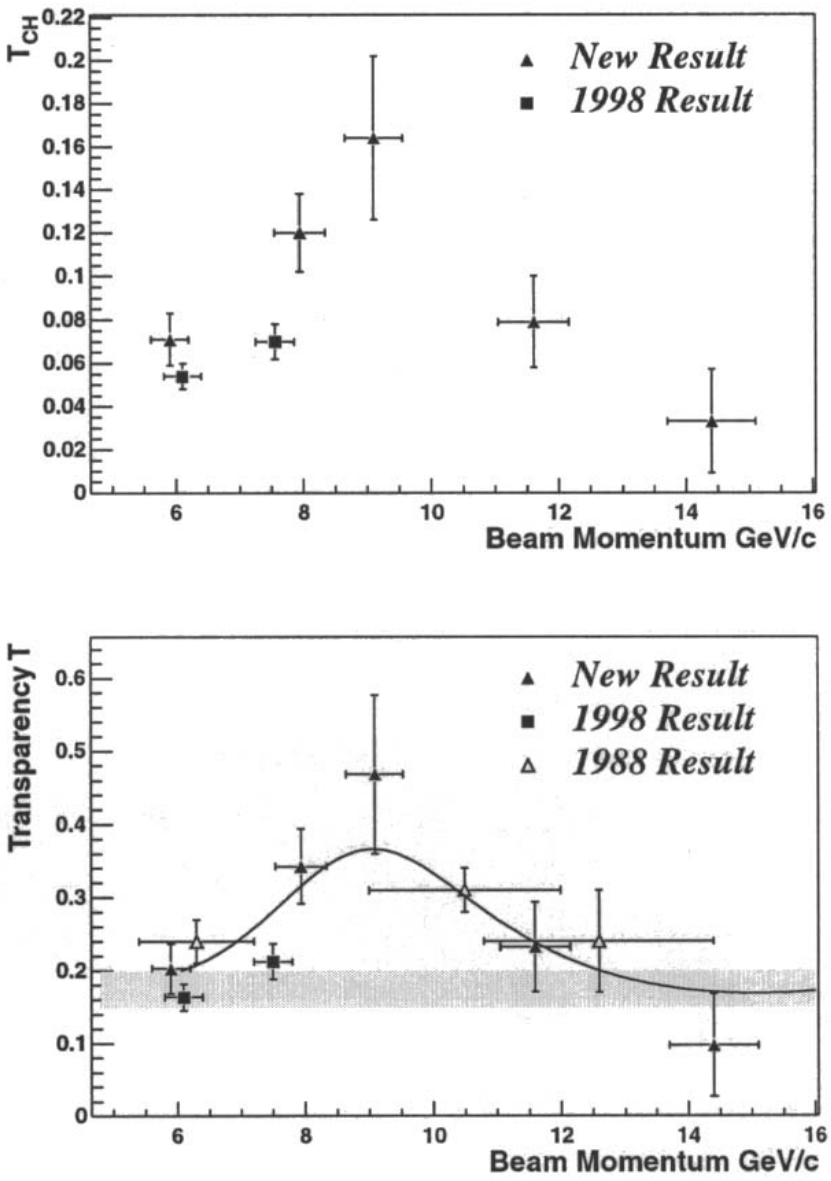

FIG. 2. Nuclear transparency as measured in the A(p,2p) precess on carbon. The shaded band represents the Glauber calculation for carbon and the solid line is the calculation from Ref. [21]

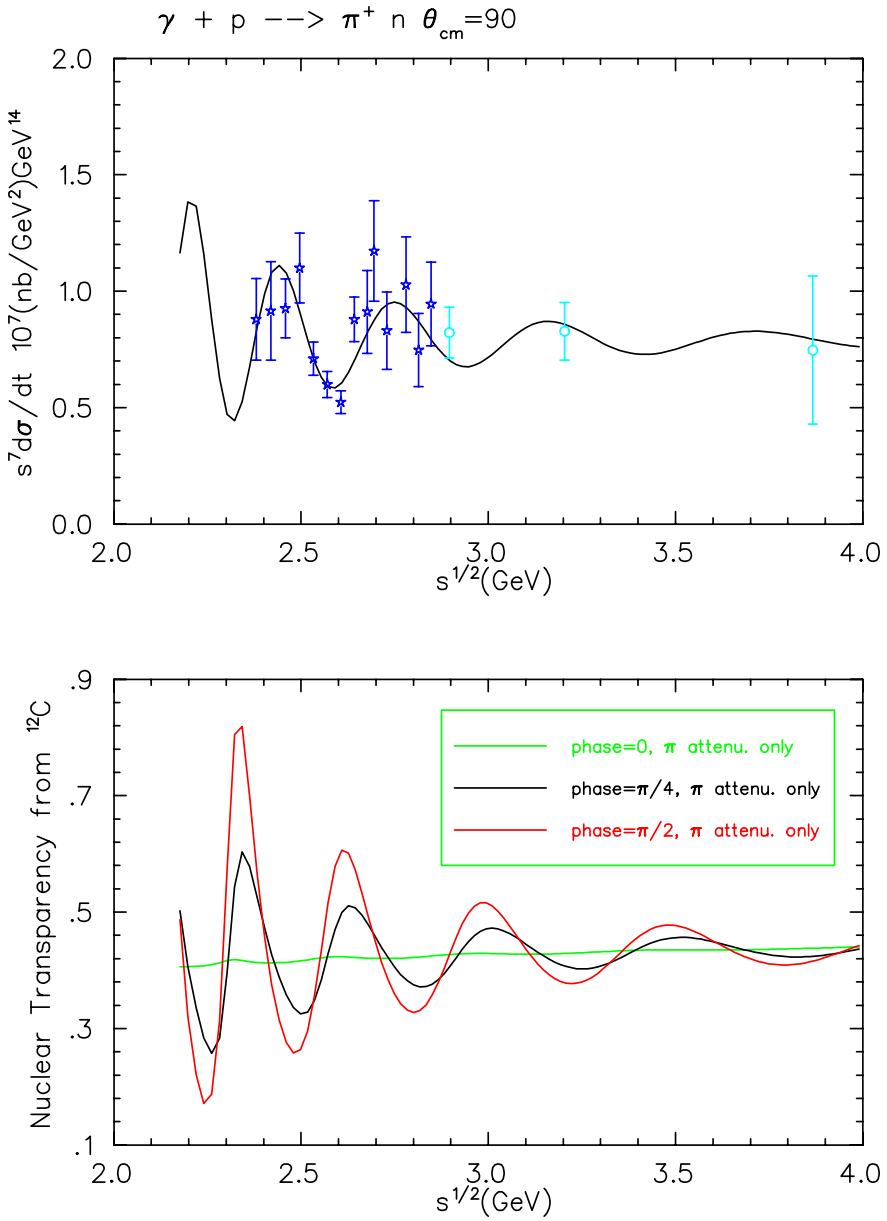

FIG. 3. The upper panel shows world data on the scaled differential cross-section $s^7 \frac{d\sigma}{dt}$ for the $\gamma p \to \pi^+ n$ process, as a function of $\sqrt{s}$ at a center-of-mass angle of 90°. The solid curve is a fit of the data based on the two-component model [24]. The lower panel shows the calculated nuclear transparency of the $\gamma p \to \pi^+ n$ process as a function of cms energy, $\sqrt{s}$ for ^{12}C, in the two-component model [24].

.

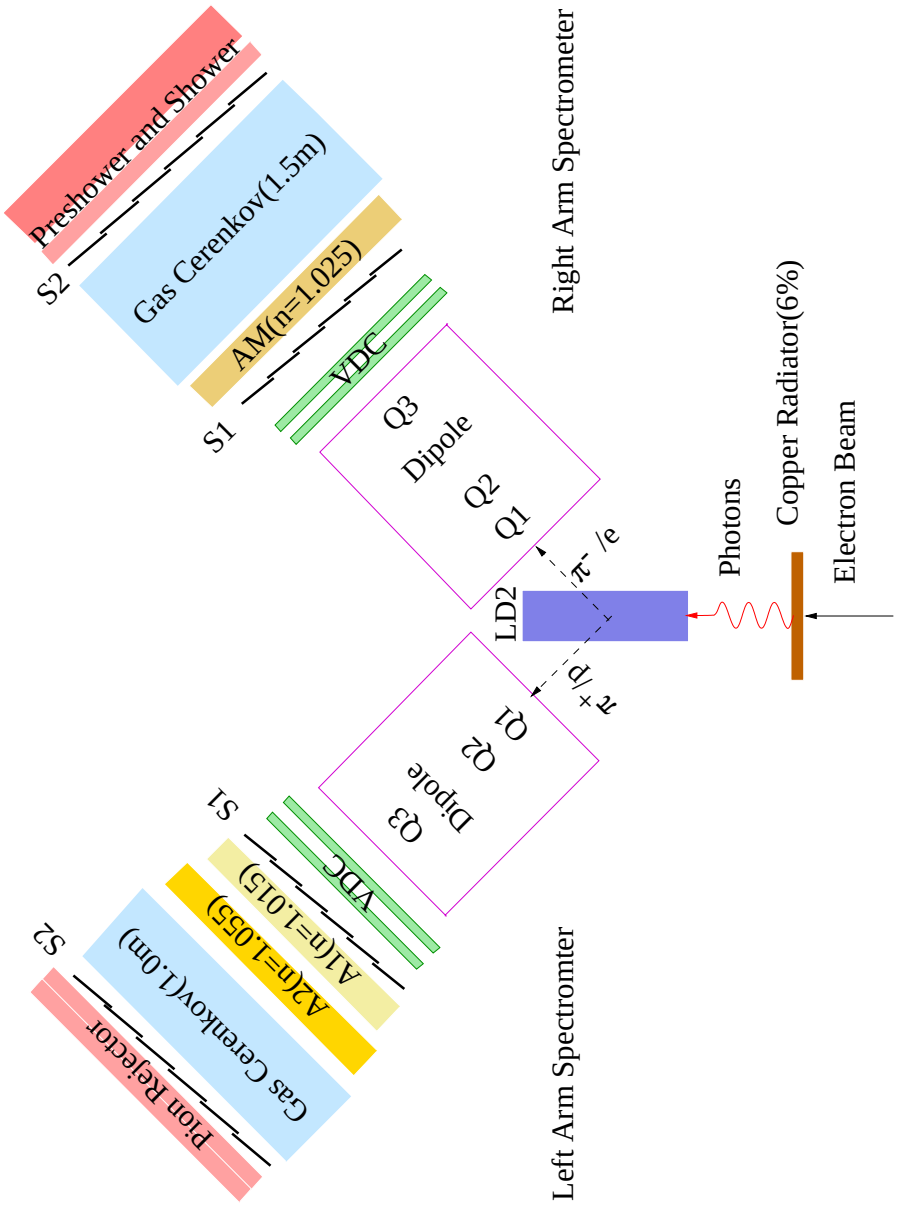

FIG. 4. The proposed experimental layout. The detector packages are identical to what had been used in E94-104.

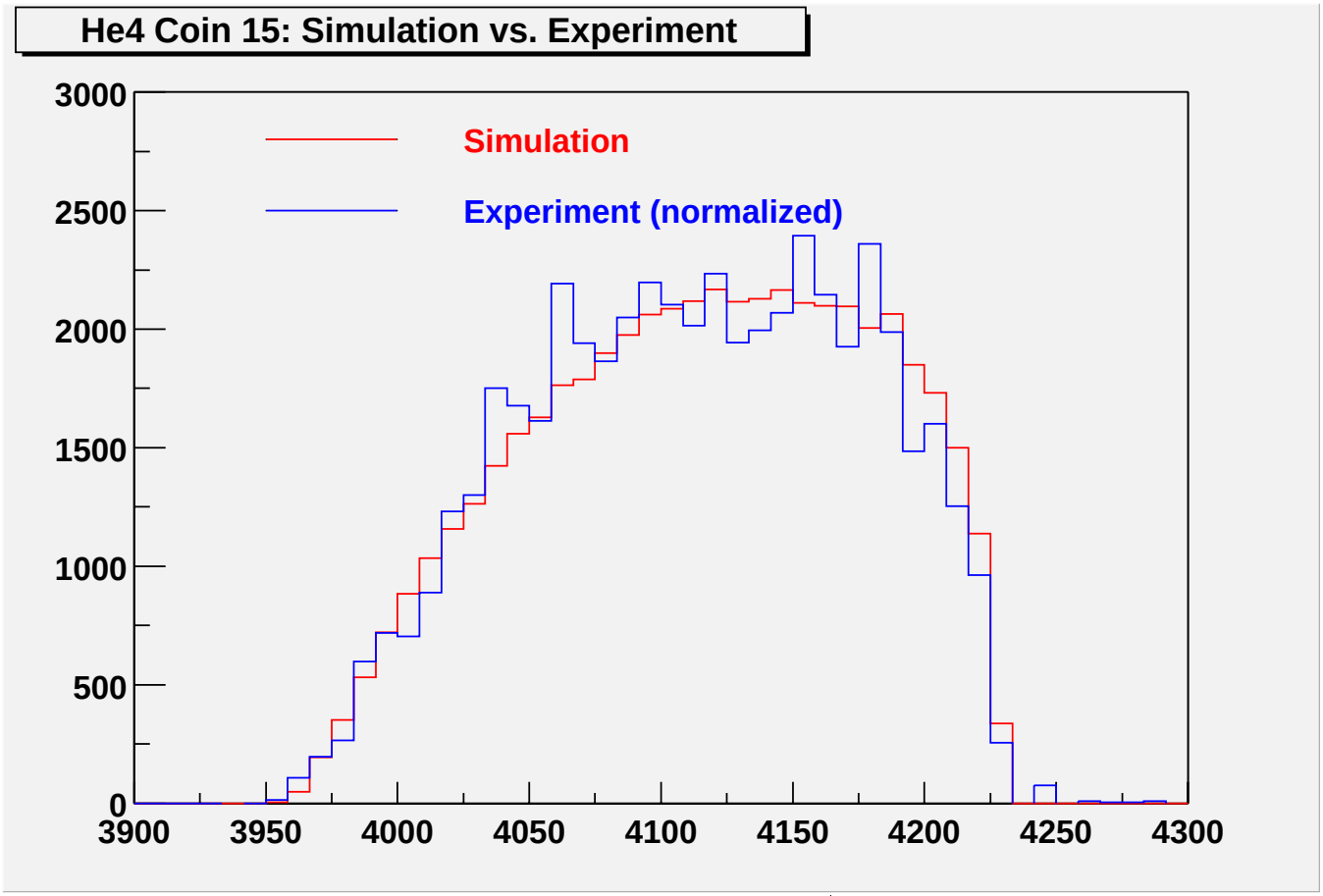

FIG. 5. The reconstructed photon energy spectrum for the ^{4}He target. The experimental reconstructed photon energy spectrum is compared with the spectrum from the Monte Carlo simulation.

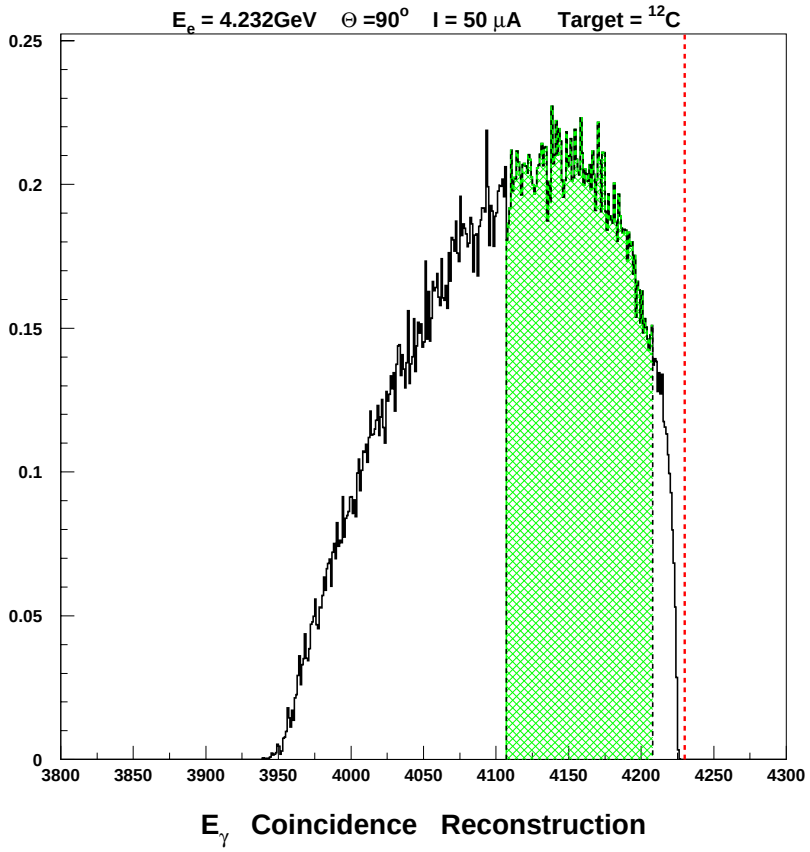

FIG. 6. The Monte Carlo simulation of the reconstructed photon energy spectrum for the ^{12}C target. The shaded region is the 100 MeV window used to determine the rates for $\sqrt{s}$ >2.8 GeV and the red dashed line represents the end point energy.

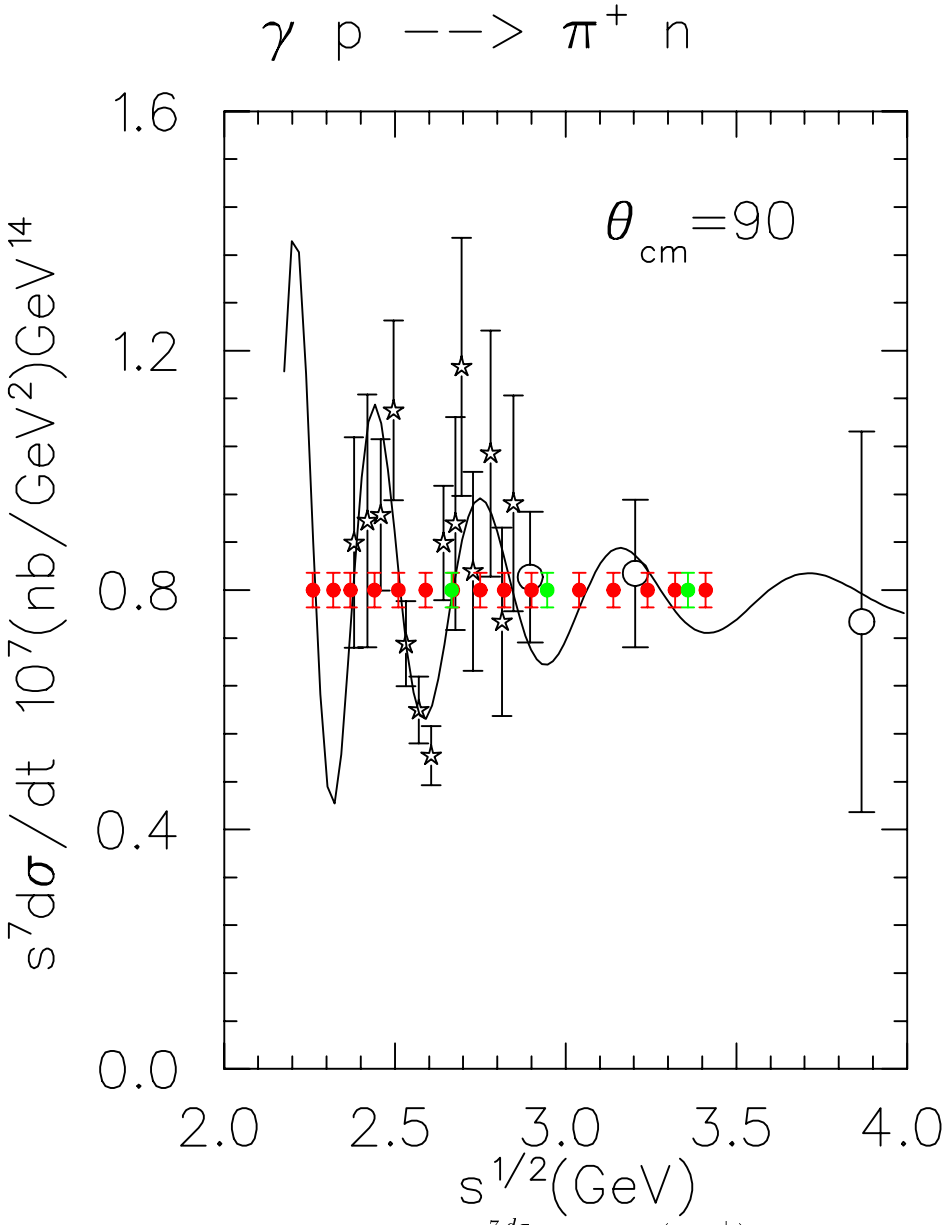

FIG. 7. The scaled differential cross-section $s^7 \frac{d\sigma}{dt}$ for the $p(\gamma, \pi^+)n$ process at C.M. angle of 90°, as a function of cms energy $\sqrt{s}$ in GeV along with the projected measurements for this experiment (red solid points). A 2% statistical uncertainty and a point-to-point 3% systematic uncertainty added in quadrature is shown in the projection. The green solid points show the completed E94-104 data points with the expected statistical uncertainty and a 3% point-to-point systematic uncertainty added in quadrature. The solid curve is the same as in Fig. 3 (upper panel).

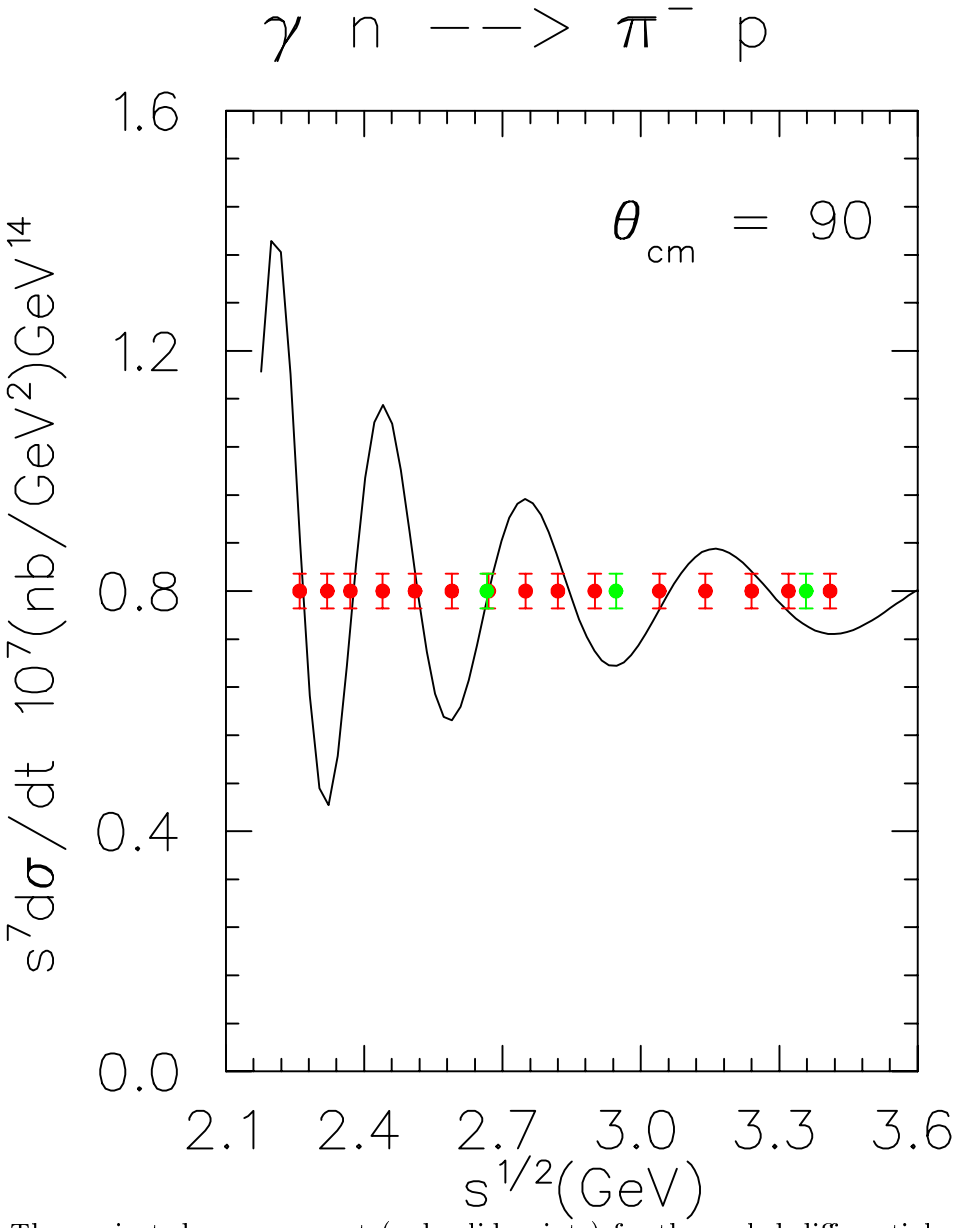

FIG. 8. The projected measurement (red solid points) for the scaled differential cross-section for the process $n(\gamma, \pi^- p)$ as a function of cms energy $\sqrt{s}$ in GeV. A 2% statistical uncertainty and a point-to-point 3% systematic uncertainty added in quadrature is shown in the projection. The green solid points show the completed E94-104 data points with the expected statistical uncertainty and a 3% point-to-point systematic uncertainty added in quadrature. The solid curve is the same as in Fig. 3 (upper panel).

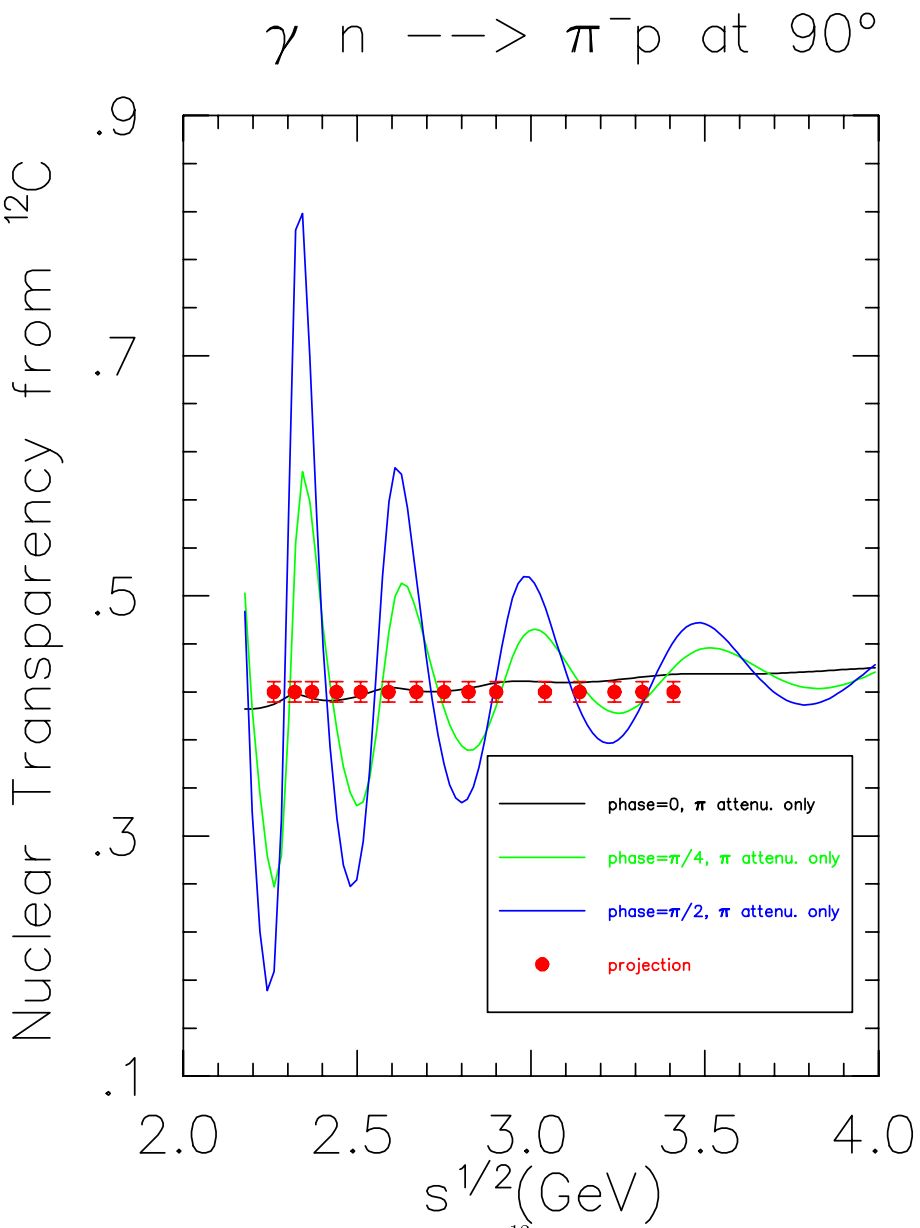

FIG. 9. The predicted nuclear transparency for ^{12}C as a function of cms energy $\sqrt{s}$ in GeV along with the projected measurements. A 2% statistical uncertainty and a systematic uncertainty of 3% added in quadrature is shown in the projection. The two-component model prediction by Jain, Kundu and Ralston [24] for phase=0, 45° and 90° are shown as black, green and blue curve, respectively.

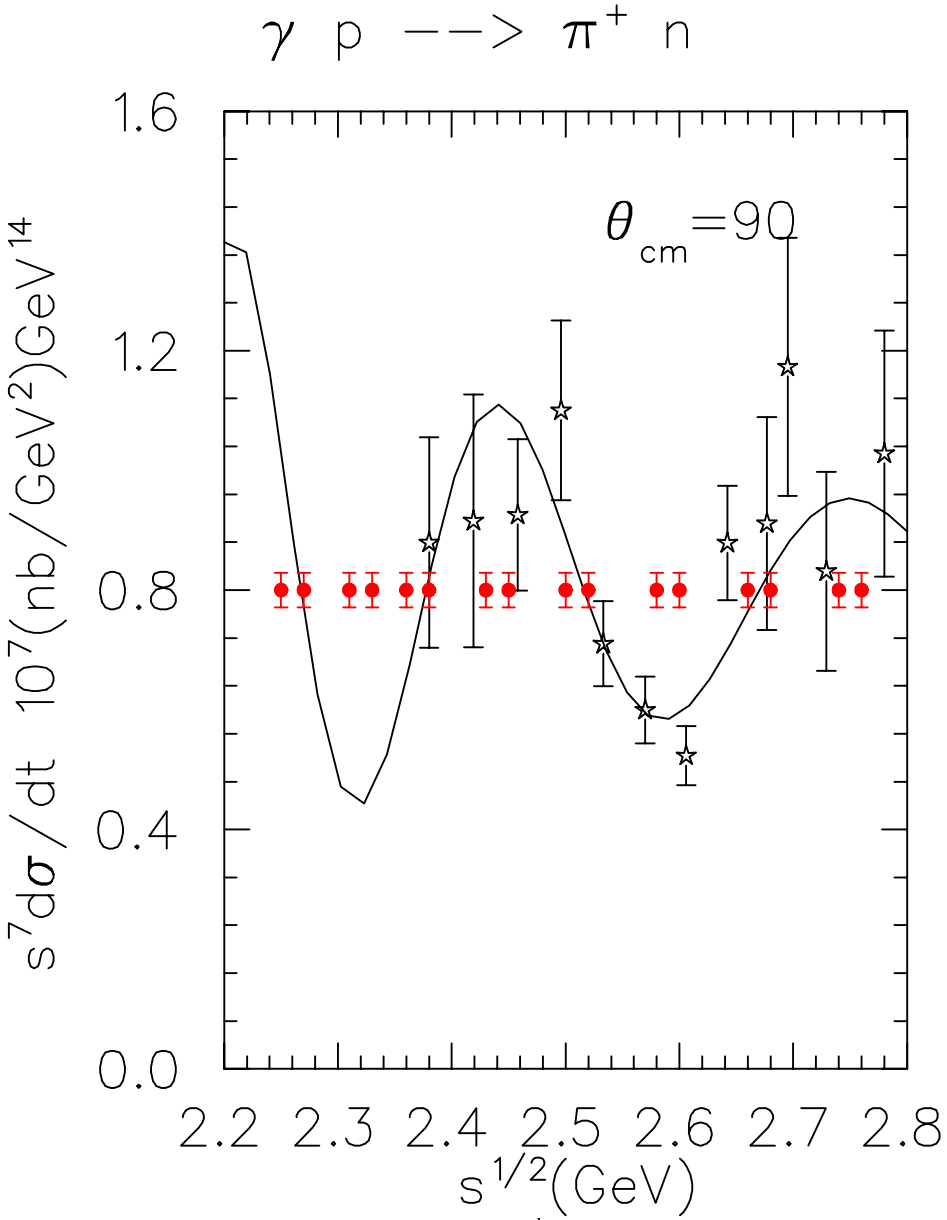

FIG. 10. The scaled differential cross-section $s^7 \frac{d\sigma}{dt}$ for the $p(\gamma, \pi^+)n$ process at C.M. angle of 90°, as a function of cms energy $\sqrt{s}$ in GeV along with the projected measurements for this experiment (red solid points). A 2% statistical uncertainty and a point-to-point 3% systematic uncertainty added in quadrature is shown in the projection. The solid curve is the same as in Fig. 3(upper panel). The $\sqrt{s} < 2.8$ GeV region is shown where the useful photon energy bin can be split to obtain a finer mapping of the oscillatory behavior.

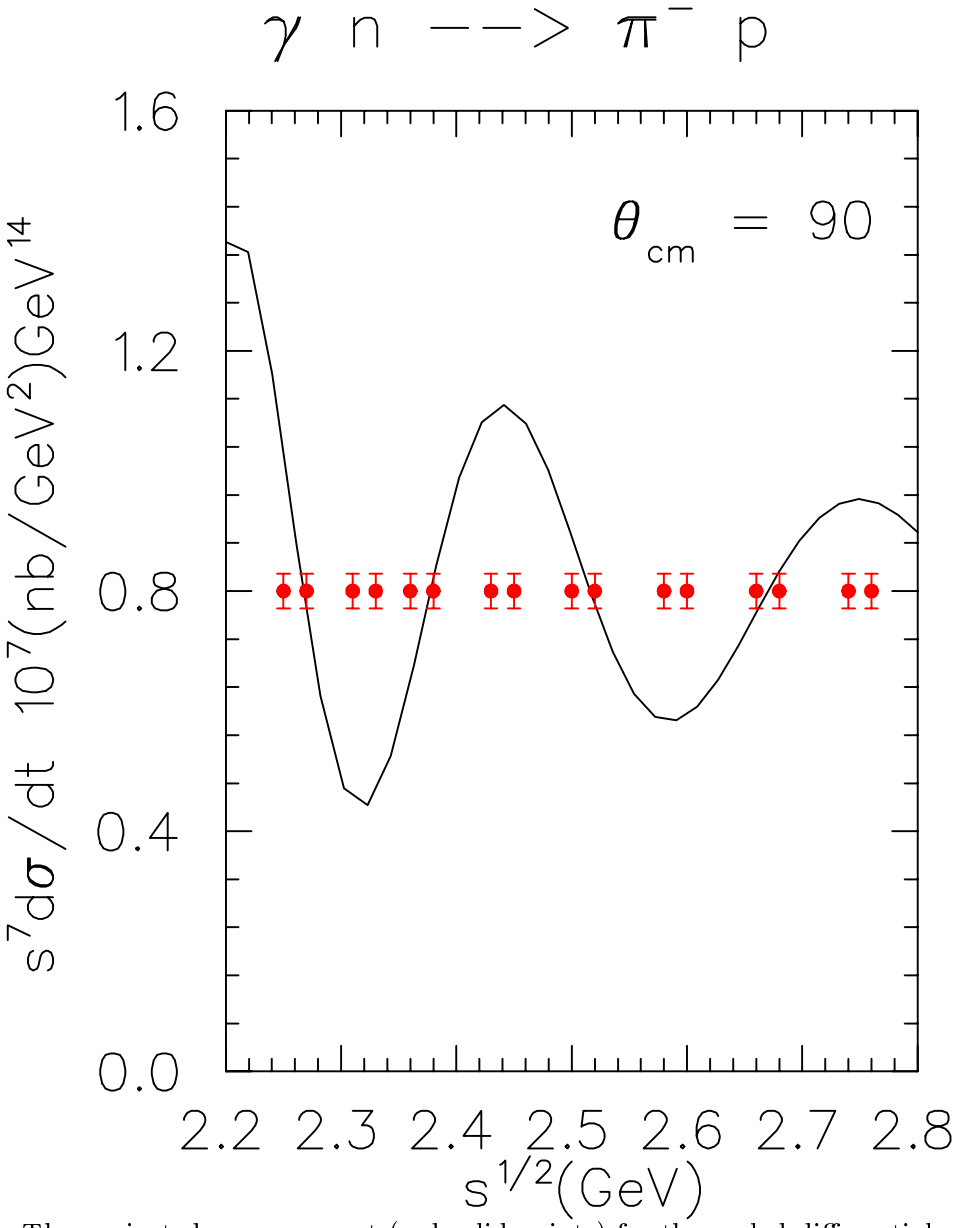

FIG. 11. The projected measurement (red solid points) for the scaled differential cross-section for the process $n(\gamma, \pi^- p)$ as a function of cms energy $\sqrt{s}$ in GeV. A 2% statistical uncertainty and s point-to-point 3% systematic uncertainty added in quadrature is shown in the projection. The solid curve is the same as in Fig. 3(upper panel). The $\sqrt{s} < 2.8$ GeV region is shown where the useful photon energy bin can be split to obtain a finer mapping of the oscillatory behavior.

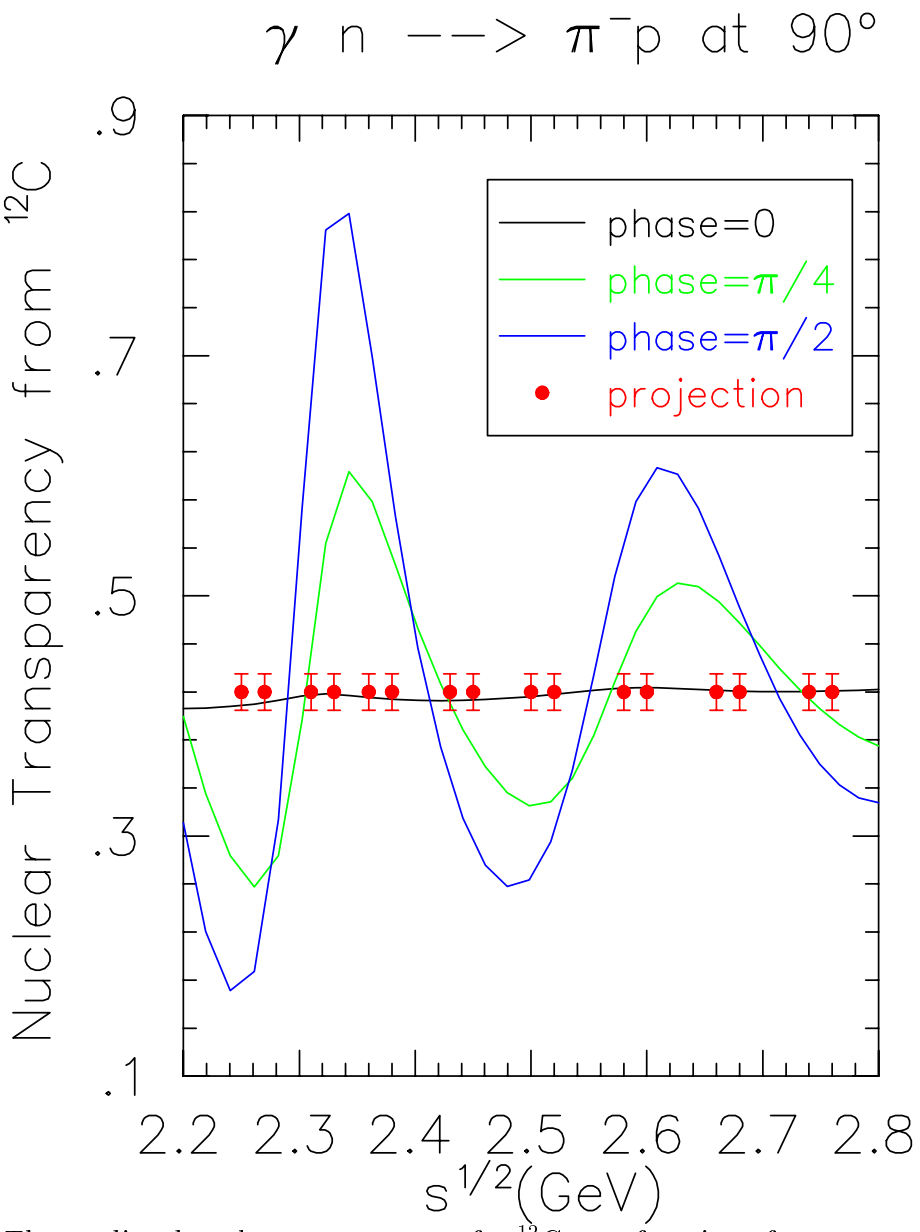

FIG. 12. The predicted nuclear transparency for ^{12}C as a function of cms energy $\sqrt{s}$ in GeV along with the projected measurements. The statistical uncertainty and a 3% systematic uncertainty added in quadrature is shown in the projection. The two-component model prediction by Jain, Kundu and Ralston [24] for phase=0, 45° and 90° are shown as black, green and blue curve, respectively. The $\sqrt{s} < 2.8$ GeV region is shown where the useful photon energy bin can be split to obtain a finer mapping of the oscillatory behavior.

TABLES

TABLE I. Table of kinematics for the $p(\gamma,\pi^+)n$ reaction at pion C.M. angle of 90^o. The photon energy listed is 75 MeV less than the electron beam energy.

E_{beam}	E_γ	$\sqrt{s}$	θ_{π^+} (lab)	P_{π^+}
GeV	GeV	GeV	deg	GeV/c
2.328	2.253	2.26	44.77	1.3192
2.474	2.399	2.32	43.74	1.3948
2.599	2.524	2.37	42.92	1.4592
2.778	2.704	2.44	41.81	1.5513
2.963	2.888	2.51	40.76	1.6459
3.180	3.106	2.59	39.61	1.7569
3.405	3.330	2.67	38.52	1.8711
3.636	3.561	2.75	37.49	1.9886
3.844	3.769	2.82	36.64	2.0941
4.088	4.013	2.90	35.70	2.2176
4.531	4.456	3.04	34.17	2.4418
4.860	4.785	3.14	33.15	2.6080
5.200	5.125	3.24	32.19	2.7795
5.480	5.405	3.32	31.46	2.9204
5.802	5.727	3.41	30.67	3.0829

TABLE II. Table of kinematics for the quasifree $n(\gamma,\pi^-p)$ reaction at pion C.M. angle of 90^o. The photon energy listed is 75 MeV less than the electron beam energy.

E_{beam}	E_γ	$\sqrt{s}$	θ_{π^-} (lab)	θ_p (lab)	P_{π^-}	P_p
GeV	GeV	GeV	deg	deg	GeV/c	GeV/c
2.328	2.253	2.26	44.77	35.22	1.3192	1.6111
2.474	2.399	2.32	43.74	34.72	1.3948	1.6930
2.599	2.524	2.37	42.92	34.32	1.4592	1.7623
2.778	2.704	2.44	41.81	33.76	1.5513	1.8610
2.963	2.888	2.51	40.76	33.21	1.6459	1.9618
3.180	3.106	2.59	39.61	32.59	1.7569	2.0795
3.405	3.330	2.67	38.52	31.99	1.8711	2.2000
3.636	3.561	2.75	37.49	31.40	1.9886	2.3233
3.844	3.769	2.82	36.64	30.90	2.0941	2.4336
4.088	4.013	2.90	35.70	30.33	2.2176	2.5624
4.531	4.456	3.04	34.17	29.38	2.4418	2.7949
4.860	4.785	3.14	33.15	28.73	2.6080	2.9667
5.200	5.125	3.24	32.19	28.10	2.7795	3.1432
5.480	5.405	3.32	31.46	27.61	2.9204	3.2879
5.802	5.727	3.41	30.67	26.08	3.0829	3.4544

TABLE III. Table of central photon energies and $\sqrt{s}$ when the 100 MeV bin between 25 and 125 MeV below the end point energy is divided into 2 bins.This will be done for $\sqrt{s} < 2.8$ GeV.

E_{beam}	$E_\gamma(1)$	$E_\gamma(2)$	$\sqrt{s}(1)$	$\sqrt{s}(2)$
GeV	GeV	GeV	GeV	GeV
2.328	2.228	2.278	2.25	2.27
2.474	2.374	2.424	2.31	2.33
2.599	2.499	2.549	2.36	2.38
2.778	2.679	2.729	2.43	2.45
2.963	2.863	2.913	2.50	2.52
3.180	3.081	3.131	2.58	2.60
3.405	3.305	3.355	2.66	2.68
3.636	3.536	3.586	2.74	2.76

TABLE IV. Estimated rates for LH2 (singles), LD2 (coincidence) and ^{12}C (coincidence) in a 50 MeV photon energy window for $\sqrt{s} < 2.8$ GeV and a 100 MeV window for $\sqrt{s} > 2.8$ GeV, starting 25 MeV below the end point energy.

$\sqrt{s}$	LH2 rates	LD2 rates	^{12}C rates
GeV	Hz	Hz	Hz
2.26	237.7	30.1	1.03
2.32	177.2	23.2	0.85
2.37	126.7	17.5	0.70
2.44	97.6	13.4	0.54
2.51	75.4	10.1	0.41
2.59	50.0	6.2	0.26
2.67	24.9	2.3	0.10
2.75	30.5	1.20	0.06
2.82	21.6	2.07	0.10
2.90	11.7	1.68	0.08
3.04	7.6	1.16	0.064
3.14	5.8	0.90	0.055
3.24	4.1	0.65	0.046
3.32	2.2	0.45	0.039
3.41	1.3	0.22	0.031

TABLE V. Estimated singles rates for LD2 in a 100 MeV photon energy window starting 25 MeV below the end point energy.

$\sqrt{s}$	$d(\gamma,\pi^-)$ rates	$d(\gamma,p)$ rates	accidental	e^-/π^-(LD2)	e^-/π^-(LH2)
GeV	Hz	Hz	Hz		
2.26	27.5	863.2	8.8E-03	0.45	47.4
2.32	14.1	987.1	4.5E-03	0.49	46.8
2.51	11.0	799.6	3.6E-03	0.56	42.2
2.67	4.8	416.3	1.7E-03	0.62	38.1
2.82	1.6	269.5	0.6E-03	0.75	32.2
3.04	0.8	131.4	0.4E-03	0.87	27.1
3.24	0.4	62.3	1.7E-04	0.95	23.9
3.41	0.2	3.5	1.1E-04	1.01	21.5

TABLE VI. Estimated beam time requirements for the LH2, LD2, and ^{12}C targets.

$\sqrt{s}$	LH2 beam time	LD2 beam time	^{12}C beam time	Total
GeV	hours	hours	hours	hours
2.26	0.5	0.5	1.0	2.0
2.32	0.5	0.5	1.0	2.0
2.37	0.5	0.5	1.0	2.0
2.44	0.5	0.5	1.5	2.5
2.51	0.5	0.5	2.0	3.0
2.59	0.5	0.5	2.5	3.5
2.67	0.5	0.5	7.0	8.0
2.75	0.5	0.5	12.5	13.5
2.82	0.5	0.5	7.0	8.0
2.90	0.5	0.5	8.5	9.5
3.04	0.5	1.0	11.0	12.5
3.14	0.5	1.0	13.0	14.5
3.24	0.5	1.5	15.0	17.0
3.32	0.5	2.0	18.0	20.5
3.41	1.0	3.5	23.0	27.5
Total Radiator IN	8.0	14.0	124.0	146.0
Radiator OUT	2.0	5.0	42.0	49.0
Background Studies	5	15		20
Total				215
Overhead				90+20+8
Grand Total	15.0	34.0	166.0	333 ($\sim$ 14 days)

REFERENCES

[1] G. White *et al.*, Phys. Rev. **D49**, 58 (1994).
[2] S.J. Brodsky and G.R. Farrar, Phys. Rev. Lett.**31**, 1153 (1973); Phys. Rev. D **11**, 1309 (1975); V. Matveev *et al.*, Nuovo Cimento Lett. **7**, 719 (1973);
[3] G.P. Lepage, and S.J. Brodsky, Phys. Rev. D **22**, 2157 (1980).
[4] N. Isgur and C. Llewelyn-Smith, Phys. Rev. Lett. **52**, 1080 (1984).
[5] J. Napolitano *et al.*, Phys. Rev. Lett. **61**, 2530 (1988); S.J. Freedman *et al.*, Phys. Rev. C **48**, 1864 (1993); J.E. Belz *et al.*, Phys. Rev. Lett. **74**, 646 (1995).
[6] C. Bochna *et al.*, Phys. Rev. Lett. **81**, 4576 (1998).
[7] E.C. Schulte, *et al.*, Phys. Rev. Lett. **87**, 102302 (2001);
[8] K. Wijesooriya, *et al.*, JournalPhys. Rev. Lett.86, 2975 (2001).
[9] D. P. Owen *et al.*, Phys. Rev. **181**, 1794 (1969); K. A. Jenkins *et al.*, Phys. Rev. D **21**, 2445 (1980); C. Haglin *et al.*, Nucl. Phys. B **216**, 1 (1983).
[10] R.L. Anderson *et al.*, Phys. Rev. **D14**, 679 (1976).
[11] P. V. Landshoff, Phys. Rev. D **10**, 1024 (1974).
[12] A.W. Hendry, Phys. Rev. D **10**, 2300 (1974).
[13] D.G. Crabb *et al.*, Phys. Rev. Lett. **41**, 1257 (1978).
[14] G.R. Court *et al.*, Phys. Rev. Lett. **57**, 507 (1986), T.S. Bhatia *et al.*, Phys. Rev. Lett. **49**, 1135 (1982), E.A. Crosbie *et al.*, Phys. Rev. D **23**, 600 (1981).
[15] S.J. Brodsky, C.E. Carlson, and H. Lipkin, Phys. Rev. D **20**, 2278 (1979).
[16] A. Sen, Phys. Rev. D **28**, 860 (1983).
[17] J. Botts and G. Sterman, Nucl. Phys. **B325**, 62 (1989).
[18] A. H. Mueller, Phys. Rep. **73**, 237 (1981).
[19] A.S. Carroll *et al.*, Phys. Rev. Lett. **61**, 1698 (1988).
[20] Y. Mardor *et al.*, Phys. Rev. Lett. **81**, 5085 (1998); A. Leksanov *et al.*, Phys. Rev. Lett. **87**, 212301-1 (2001).
[21] J.P. Ralston and B. Pire, Phys. Rev. Lett. **61**, 1823 (1988), J.P. Ralston and B. Pire, Phys. Rev. Lett. **65**, 2343 (1990).
[22] C.E. Carlson, M. Chachkhunashvili, and F. Myhrer, Phys. Rev. D **46**, 2891 (1992).
[23] L.L. Frankfurt, G.A. Miller, M.M. Sargsian, and M.I. Strikman, Phys. Rev. Lett. **84**, 3045 (2000), M.M. Sargsian, private communication.
[24] P. Jain, B. Kundu, and J. Ralston, hep-ph/0005126.
[25] G.R. Farrar, G. Sterman, and H. Zhang, Phys. Rev. Lett. **62**, 2229 (1989).
[26] E. Anciant *et al.*, Phys. Rev. Lett. **85**, 4682 (2000).
[27] S. J. Brodsky, and G. F. de Teramond, Phys. Rev. Lett. **60**, 1924 (1988).
[28] B. Kundu, J. Samuelsson, P. Jain and J.P. Ralston, Phys. Rev. D **62**, 113009 (2000).
[29] S.J. Brodsky and A.H. Mueller, Phys. Lett. **B 206**, 685 (1988).
[30] G.R. Farrar, H. Liu, L.L. Frankfurt, and M.I. Strikman, Phys. Rev. Lett. **61**, 686 (1988).
[31] P. Jain, B. Pire, and J.P. Ralston, Phys. Rep. **271**, 67 (1996).
[32] N.C.R. Makins *et al.*, Phys. Rev. Lett. **72**, 1986 (1994); T.G. O'Neill *et al.*, Phys. Lett. **351**, 87 (1995); D. Abbott, *et al.*, Phys. Rev. Lett. **80**, 5072 (1998); K. Garrow, *et al.*, Submitted to Phys. Rev. C.
[33] P. Jain, private communication.
[34] D. Dutta, Ph.D. Thesis, Northwestern University, Unpublished, (1999).
[35] H. Gao, R. J. Holt and V. R. Pandharipande, Phys. Rev. C **54**, 2779 (1996).

[36] H. Areti, private communication.
[37] "Photoproduction of Elementary Particles", edited by H. Genzel, P. Joos and W. Pfeil pp16-268, (1973).
[38] M. A. Shupe *et al.*, Phys. Rev. D. **19**, 1921 (1979).